5561

Fosgonimeton, a Small-Molecule Positive Modulator of the Neurotrophic Hepatocyte Growth Factor System, Inhibits LPS-Mediated Neuroinflammation in BV2 Microglia

Wei Wu, Leah G. Helton,* Sherif M. Reda, Sabrina Fechtner, Robert W. Taylor, Kevin J. Church

Athira Pharma, Bothell, WA, USA
*Formerly affiliated with Athira Pharma, Inc.

CONCLUSIONS

1. Fosgo-AM decreases mRNA expression of proinflammatory mediators (TNF-α, IL-1β, IL-6, iNOS, COX-2, and NLRP3)
2. Fosgo-AM inhibits LPS-induced activation of ERK, p38, JNK, AKT, NF-κB, and STAT3
3. Fosgo-AM attenuates LPS-induced mitochondrial dysfunction and oxidative stress

KEY TAKEAWAY

The anti-inflammatory effects of fosgo-AM highlight the therapeutic potential of fosgonimeton for the treatment of neuroinflammatory diseases

Acknowledgments

The study was sponsored by Athira Pharma, Inc. Editorial support was provided by ApotheCom and funded by Athira Pharma, Inc.

Disclosures

Wei Wu, Sherif M. Reda, Sabrina Fechtner, Robert W. Taylor, and Kevin J. Church are employees and stockholders of Athira Pharma, Inc. Leah Helton is a former employee of Athira Pharma, Inc.

Disclaimer

Fosgonimeton is an investigational therapy that has not received US Food and Drug Administration approval and has not been demonstrated to be safe or effective for any use.

Presented at Neuroscience 2023; November 11-15, 2023; Washington, DC

INTRODUCTION

- Neuroinflammation is a key pathological component of neurodegenerative diseases such as Alzheimer's disease, Parkinson's disease, multiple sclerosis, and amyotrophic lateral sclerosis
- Microglia are the brain's resident immune cells, and they promote broad-spectrum neuroinflammation when activated by pathological conditions[1]
- The neurotrophic HGF system exerts anti-inflammatory effects; therefore, positive modulation of the neurotrophic HGF system could be beneficial in counteracting neuroinflammation associated with neurodegenerative disease[2]
- Previously, we showed that fosgonimeton, a small-molecule positive modulator of the neurotrophic HGF system, decreased LPS-induced proinflammatory cytokine release in macrophages and attenuated LPS-induced deficits in vitro and vivo[3]

Figure 1. Fosgo-AM, the active metabolite of fosgonimeton, is hypothesized to inhibit inflammatory pathways in LPS-stimulated microglia

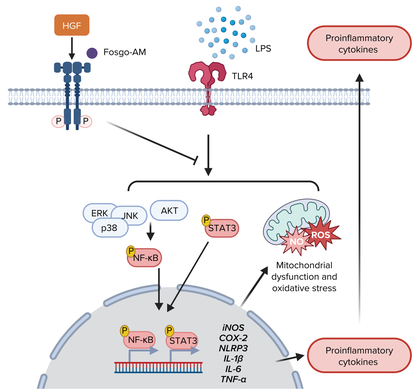

OBJECTIVE

To investigate the cellular mechanism by which fosgo-AM induces anti-inflammatory effects in BV2 microglia cells

METHODS

Gene expression assay

- BV2 cells were pretreated with LPS 1 µg/mL for 45 minutes, followed by cotreatment with fosgo-AM for 23.5 hours
- Cell lysates were used in a gene expression assay
- Luminex Quantigene 12 multiplex assay was used to evaluate the gene expression (*COX-2, GADPH, IL-1β, IL-6, iNOS, HPRT, LDHA, NLRP3, TBP, and TNF-α*)
- The data were normalized using the geometric mean of the four housekeeping genes (*GADPH, LDHA, TBP*, and *HPRT*)
- Gene expression was visualized as the mean of fold changes of mRNA levels relative to LPS vehicle

Cellular signaling pathway assay

- BV2 cells were pretreated with LPS 0.2 µg/mL for 45 minutes, followed by cotreatment with fosgo-AM 1 µM for 1 hour
- Cell lysates were analyzed via HTRF for pAKT (Ser473), pERK (Thr202/Tyr204), P-p38 (Thr180/Tyr182), pJNK (Thr183/Tyr185), pNF-κB (Ser536), pSTAT3 (Tyr705), and GAPDH
- GAPDH was used to normalize levels of phosphorylation for each protein

Mitochondria membrane potential assay

- BV2 cells were treated with LPS 1 µg/mL and cotreated with fosgo-AM 1 µM for 23.5 hours. Supernatants were then discarded and replaced by HBSS containing JC-1 dye 10 µg/mL and Hoechst 3342 1 µg/mL and incubated for 30 minutes at 37°C
- Cells were rinsed twice with HBSS before imaging on a Keyence BZ-X810 imager with a 60× oil lens
- The fluorescence ratio of at least 3000 different cells was quantified in each condition, and the mean of the ratio was generated as the value of one experiment
- The mean and SEM were analyzed from values of three independent experiments

ROS and NO production assay

- BV2 cells were treated with LPS 1 µg/mL and cotreated with fosgo-AM for 23.5 hours. Supernatants were collected for NO production measurement using the Griess Reagent System. HBSS containing DCFDA 20 µM and Hoechst 3342 1 µg/mL was added to each well and incubated for 45 minutes at 37°C
- Cells were rinsed twice with HBSS before imaging on a Keyence BZ-X810 imager with a 20× lens
- The fluorescence ratio of at least 3000 different cells was quantified in each condition, and the mean of the green fluorescence area was generated as the value of one experiment
- The mean and SEM was analyzed from values of three independent experiments

RESULTS

Figure 2. Fosgo-AM inhibits LPS-stimulated expression of proinflammatory cytokines in BV2 microglial cells

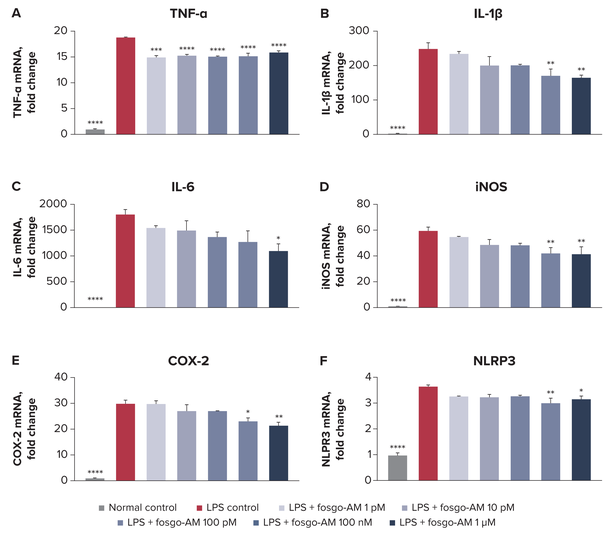

mRNA expression of proinflammatory cytokines (A) TNF-α, (B) IL-1β, and (C) IL-6 and inflammatory mediators (D) iNOS, (E) COX-2, and (F) NLRP3 in LPS-stimulated BV2 microglia in the presence or absence of fosgo-AM supplemented with 0.05 ng/mL HGF.

Data presented as mean + SEM; n = 3 biological replicates. Statistical differences were determined by one-way ANOVA followed by Dunnett's multiple comparisons test.

*p < 0.05, **p < 0.01, ***p < 0.001, ****p < 0.0001 versus LPS control.

Figure 3. Fosgo-AM decreases LPS-mediated AKT/MAPK signaling and NF-κB/STAT3 phosphorylation in BV2 microglia

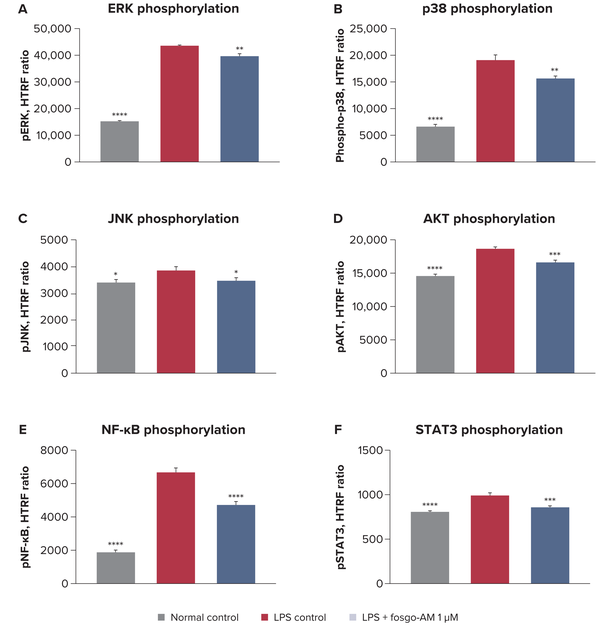

Phosphorylation of (A) ERK, (B) p38, (C) JNK, (D) AKT, (E) NF-κB, and (F) STAT3 in LPS-stimulated BV2 microglia in the presence or absence of fosgo-AM supplemented with HGF 0.05 ng/mL.

Data presented as mean + SEM; n = 6 biological replicates. Statistical differences were determined by one-way ANOVA followed by Dunnett's multiple comparisons test.

*p < 0.05, **p < 0.01, ***p < 0.001, ****p < 0.0001 versus LPS control.

Figure 4. Fosgo-AM rescues mitochondrial membrane potential after LPS exposure in BV2 microglial cells

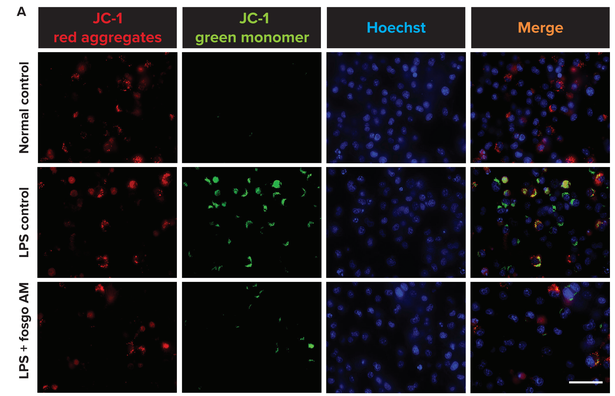

(A) Representative images of mitochondria membrane potential detected with JC-1 dye in LPS-stimulated microglia in the presenceor absence of fosgo-AM supplemented with HGF 0.05 ng/mL. Pathological reduction in mitochondrial membrane potential is visible as a conversion of red JC-1 aggregates to green JC-1 monomers. Hoechst (blue) indicates nucleus. Scale bar, 50 uM. (B) Quantification of JC-1 red/green fluorescence ratio.

Shown are the mean + SEM; n = 3 biological replicates. Statistical differences were determined by one-way ANOVA followed by Dunnett's multiple comparisons test.

*p < 0.05, **p < 0.01, ***p < 0.001, ****p < 0.0001 versus LPS control.

Figure 5. Fosgo-AM reduces oxidative stress and NO production in LPS-stimulated microglia

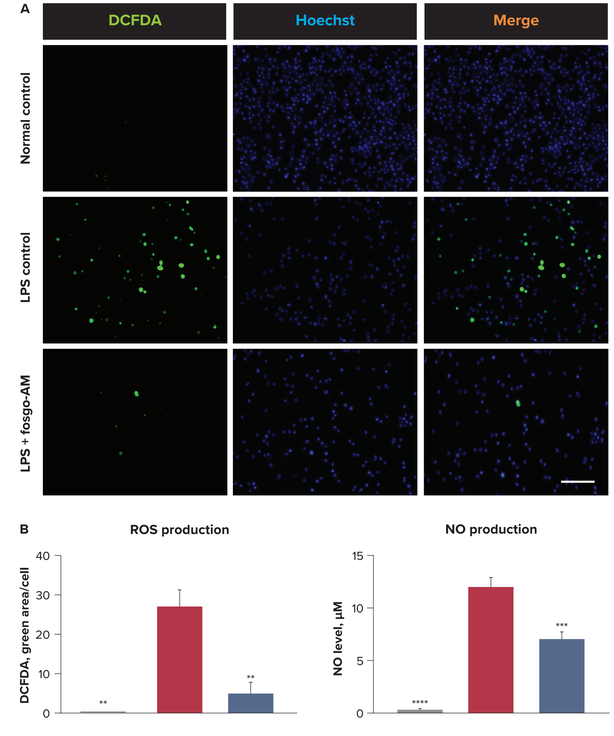

(A) Representative images of detection of ROS production with DCFDA in LPS-stimulated microglia in the presence or absence of fosgo-AM supplemented with HGF 0.05 ng/mL. DCFDA dye fluorescence (green) indicates ROS production, Hoechst dye (blue) indicates nucleus. Scale bar, 100 µM. (B) Quantification of DCFDA green fluorescence. (C) Detection of NO production from supernatant measured by the Griess Reagent System.

Shown is the mean + SEM; n = 3 biological replicates. Statistical differences were determined by one-way ANOVA followed by Dunnett's multiple comparisons test.

*p < 0.05, **p < 0.01, ***p < 0.001, ****p < 0.0001 versus LPS control.

References **1.** Muzio L et al. *Front Neurosci.* 2021;15:742065. **2.** Desole C et al. *Front Cell Dev Biol.* 2021;9:683609. **3.** Johnston JL et al. *Neurother.*. 2023;20:431-451.

Abbreviations **AKT**, protein kinase B; **ANOVA**, analysis of variance; **COX-2**, prostaglandin-endoperoxide synthase 2; **DAPI**, 4′,6-diamidino-2-phenylindole; **DCFDA**, dichlorodihydrofluorescein diacetate; **ERK**, extracellular signal–regulated kinase; **fosgo-AM**, active metabolite of fosgonimeton; **GAPDH**, glyceraldehyde 3-phosphate dehydrogenase; **HBSS**, Hanks' balanced salt solution; **HGF**, hepatocyte growth factor; **HPRT**, hypoxanthine-guanine phosphoribosyltransferase; **HTRF**, homogeneous time resolved fluorescence; **IL-1β**, interleukin 1 beta; **IL-6**, interleukin 6; **iNOS**, inducible nitric oxide synthase; **JC-1**, 5,5,6,6′-tetrachloro-1l′,3,3′ tetraethylbenzimi-dazoylcarbocyanine iodide; **JNK**, c-Jun N-terminal kinase; **LDHA**, lactate dehydrogenase A; **LPS**, lipopolysaccharide; **MAPK**, mitogen-activated protein kinase; **mRNA**, messenger ribonucleic acid; **NF-κB**, nuclear factor kappa-light-chain-enhancer of activated B cells; **NLRP3**, NLR family pyrin domain containing 3; **NO**, nitric oxide; **P**, phosphorylation; **p38**, mitogen-activated protein kinase; **pAKT**, phosphorylated protein kinase B; **pERK**, phosphorylated extracellular signal–regulated kinase; **pJNK**, phosphorylated Jun-amino-terminal kinase; **pNF-κB**, phosphorylated nuclear factor kappa B; **pSTAT3**, phosphorylated signal transducer and activator of transcription 3; **ROS**, reactive oxygen species; **SEM**, standard error of the mean; **STAT3**, signal transducer and activator of transcription 3; **TBP**, TATA binding protein; **TLR4**, toll-like receptor 4; **TNF-α** , tumor necrosis factor α.